Modeling of Bearingless Switched Reluctance Motor Based on Artificial Neural Network

Cai Jun[1,a], Deng Zhiquan[1], Qi Ruiyun[1], Liu Zeyuan[1]

[1]Nanjing University of Aeronautics and Astronautics, Nanjing, 210016, China
[a]jcai_yjs05@126.com

Abstract: Accurately calculating and modeling of the flux linkage characteristics is a critical step in design and analysis of optimal control strategies for Bearingless Switched Reluctance Motor (BSRM). But due to the highly nonlinear characteristics of BSRM, it is very difficult to derive a comprehensive mathematical model to satisfy the overall characteristics of the machine. To overcome this problem, in this paper, an edge finite element method (EFE) based 3-D FEM and a new enhanced incremental energy method were utilized for calculating the flux linkage characteristics; using the calculated flux data, an adaptive neural fuzzy inference system (ANFIS) based flux model was developed. Simulation results are presented and compared with the analytical nonlinear modeling method, which verified that the proposed model can modeling the BSRM more accurately and adaptively.

Keywords: Bearingless Switched Reluctance Motors, FEM, Modeling, FluxLinkage, ANFIS

Introduction

Bearingless switched reluctance motor(BSRM) combines merits of switched reluctance motor (SRM) and magnetic bearings, such as simple structure, ruggedness, robustness, frictionless, non lubrication and fault tolerant capability, which making it more suitable for high speed operation.

BSRM has two kinds of stator windings composed of main- and suspended windings, which can produce the torque and radial force simultaneously. Due to the doubly salient structure of the BSRM, in operation process, the flux varied periodically with severely local saturation. The coupling between main- and suspended windings results in more complicated distributions of magnetic field comparing to switched reluctance motor (SRM). Thus, modeling of flux linkage characteristics of BSRM is by no means a trivial task.

Researches have been done for BSRM in linear mathematical model [1]. However, the literatures investigating the nonlinear electromagnetism modeling of BSRM are less. Several attempts have been made to model the nonlinear magnetic characteristics of the SRM. Some are based on analytical model [2], which always suffers from lack of accuracy. While some others based on finite element method [3]. Although to some extent accurate, are complicated and time consuming. The capability to accommodate nonlinear modeling has made artificial neural networks ideal candidates to solve this problem [4]-[6].

In this paper, a 3-D FEA model based on edge finite element method (EFE) was developed for obtaining the distributions of SRM magnetic field, then the flux linkage characteristics were accurately calculated using enhanced incremental energy method (EIEM). In order to enhance modeling accuracy of the nonlinear flux linkage, an adaptive neural fuzzy inference system is used for approximating, based on the calculated flux linkage data. The developed model was validated via Matlab/Simulink. Simulation results show the developed models based on ANFIS are more robust and adaptive.

Basic Principle of BSRM

Fig.1 shows the A-phase winding configuration and the principle of radial force production in BSRM. The motor main winding N_{ma} consists of four coils in series, and the radial force windings N_{sa1} (α) and N_{sa2} (β) consist of two coils each. The B-phase and C-phase winding configuration is similar to that of the A-phase winding. The rotor angular position θ is defined as $\theta = 0$ at the aligned position of the A phase.

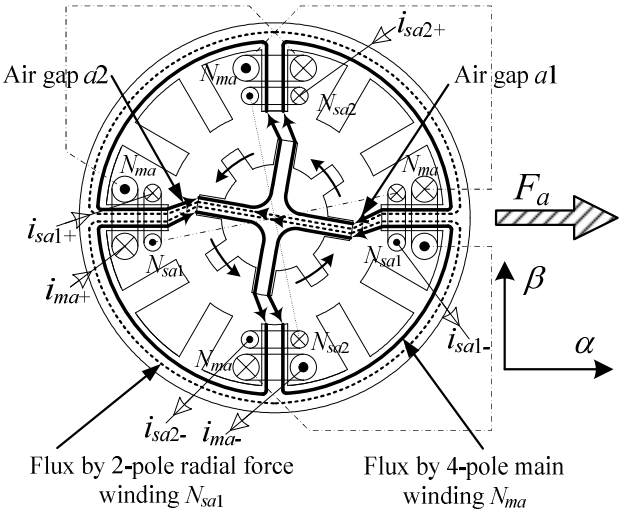

Fig.1 A-phase winding configuration.

The symmetrical two-pole fluxes (the broken lines) produced by the radial force winding current i_{sa1} break the balance of the symmetrical four-pole fluxes (the thick solid lines) produced by the main winding current i_{ma}, which results in the radial force F_a acting on rotor toward the positive direction in the α axis. A radial force F_a toward the negative direction in the α axis can be produced with a negative current i_{sa1}. Moreover, a radial force in the β axis can be produced by two-pole radial force winding current i_{sa2}. Therefore, radial force can be produced in any direction, and this principle can be applied to the B and C phase. The radial force can be continuously generated by three phases for every 15°, such as from the start of overlap and up to the aligned positions.

3-D FEA Based On Edge Finite Element Method

As discussed in our past paper [1], three different 3-D Finite element methods such as DSMP, MVP and EFE were investigated and compared, the results show that the EFE method has highest computational precision comparing with other two methods, and the DSMP method has the advantage of small computational scale, while the MVP method is not suitable for 3-D FEA. In this paper, for accurately calculating the flux linkage characteristics, the EFE based 3-D FEA is utilized.

The EFE method takes line integral of magnetic vector potential along edge or magnetic field intensity as the DOF. The DOF is always defined along the tangent direction of edge; no restriction for vertical component is imposed on the interface.

Here, the linear integral of magnetic vector potential $\boldsymbol{A}$ along edge is chosen as the DOF

$$\int \boldsymbol{N}_i \cdot d\boldsymbol{l}_j = \begin{cases} 1 & i = j \\ 0 & i \neq j \end{cases} \tag{1}$$

where, $\boldsymbol{N_i}$ is the shape function of *i*-th edge. $\boldsymbol{A}$ can be expressed as

$$\boldsymbol{A} = \sum_{i=1}^{n_e} \boldsymbol{N}_i A_i \tag{2}$$

where A_i is the linear integral of A along *i*-th edge; n_e is edge number of edge element *e*.

Therefore, the boundary value problem of BSRM with the FEE method can be obtained

$$\begin{cases} \nabla \times \dfrac{1}{\mu} \nabla \times \boldsymbol{A} = \boldsymbol{J}_S \\ \boldsymbol{A} = \sum_{i=1}^{n_e} \boldsymbol{N}_i A_i \\ A_i \big|_{S_1, S_2} = 0 \end{cases} \tag{3}$$

Based on EFE method, the 3-D magnetic density distributions are obtained. Fig. 2 shows the flux density distributions on aligned position and unaligned position respectively.

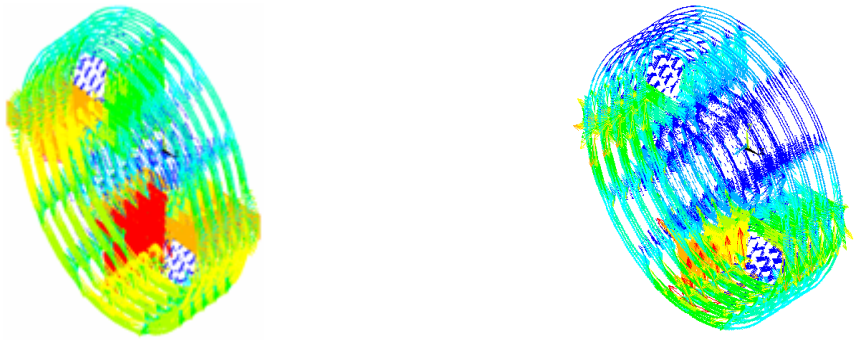

(a) (b)

Fig. 2 Flux density distribution (a) θ=0° aligned position; (b) θ=-22.5° unaligned position

Calculation of Flux Linkage Characteristics

The enhanced incremental energy method (EIEM) was applied for calculating the dynamic and static inductances in [7]. The results indicated that this method has a merit of high precision and less calculation work. In this paper, the flux linkage of main- and suspended winding were calculated by using EIEM.

The incremental energy of magnetic field can be obtained by integrating of flux density *B* and incremental magnetic field ΔH

$$\Delta W_C = \int B(\Delta H) \mathrm{d}V \tag{4}$$

And the flux linkage can be defined as

$$\Psi = \frac{\Delta W_C}{\Delta i} \tag{5}$$

The computational results of flux linkage for main- and suspended windings are shown in Fig.3.

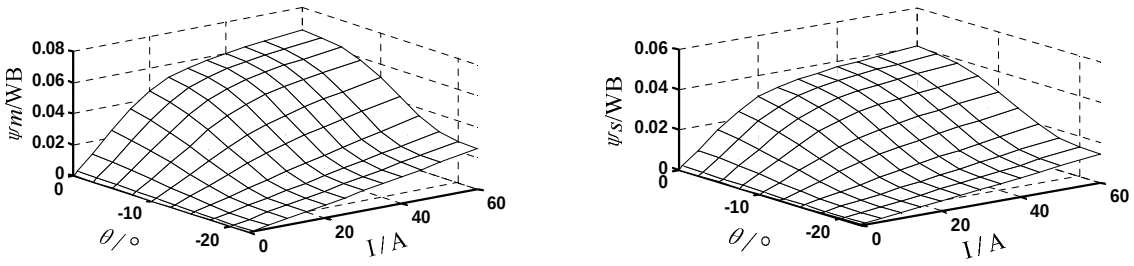

(a) (b)

Fig. 3 The calculated flux linkage characteristics (a) main winding flux linkage; (b) suspended winding flux linkage

Modeling of the Flux Linkage Characteristics Based on ANFIS

As shown in Fig. 3, the flux-linkage appears to be a complex nonlinear function of both the phase current and rotor position. Though accurately modeling of SRM is cumbersome, it can be grouped as function approximation problems.

Adaptive Neural Fuzzy Inference System. The adaptive neural fuzzy inference system (ANFIS) is implemented in the framework of adaptive networks using a hybrid learning procedure, whose membership function parameters are tuned using a back-propagation algorithm combined with a least square method, so ANFIS combines the benefits of BPNN and fuzzy logic algorithm. ANFIS is capable of dealing with uncertainty and imprecision of human knowledge, which has self-organized ability and inductive inference function to learn from the data. Hence, it is no doubt an excellent function approximation tool.

ANFIS is a multilayer feed-forward network. Each node of the network performs a particular function on incoming signals as well as a set of parameters pertaining to this node. A simple multilayer architecture of ANFIS is shown in Fig. 4.

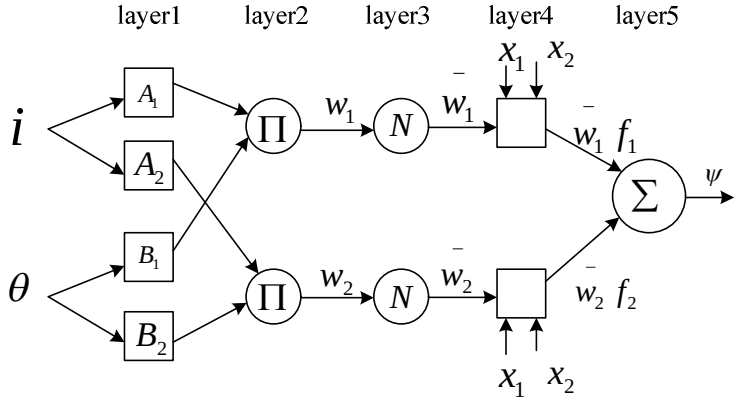

Fig. 4 A simple multilayer architecture of ANFIS

ANFIS implements a first-order Sugeno-style fuzzy system, which can be expressed as

Rule i: If x is A_i and y is B_i, then $f_i=p_ix+ q_iy+r_i$.

where A_i and B_i are the fuzzy sets in the antecedent, and p_i , q_i and r_i are the design parameters that are determined by the training process.

As shown in Fig.6, the ANFIS is formed with five layers. The detailed explanation of each layer is as follows:

Layer 1: Every node i in this layer is a square node with a node function

$$O_{1,i} = \mu_{Ai}(x_1), i = 1,2 \tag{6}$$

$$O_{1,i} = \mu_{B(i-2)}(x_2), i = 3,4 \tag{7}$$

where x_i(i=1,2) is the input of the node i; A_i or $B_{(i-2)}$ are the linguistic label correlated with the node function. While $O_{1,i}$ is the degree of membership function of the fuzzy set A. Usually we choose $\mu_{Ai}(x)$ to be bell-shaped with maximum equal to 1 and minimum equal to 0, such as

$$\mu_{Ai}(x) = \exp\left\{-\left(\frac{x - c_i}{a_i}\right)^2\right\} \tag{8}$$

where ($a_{i,}$, c_i) is the parameter set. As the values of these parameters change, the bell shape functions vary accordingly. In this paper, function (8) is chosen as the input membership function.

Layer 2: Every node of this layer calculates the firing strength of a rule by multiplying the degree of membership function. For instance

$$O_{2,i} = \mu_{Ai}(x_1) \times \mu_{Bi}(x_2), i = 1,2 \tag{9}$$

Layer 3: Every node in this layer is a circle node labeled N. The ith node calculates the ratio of the ith rule's firing strength to the sum of all rules' firing strengths:

$$O_{3,i} = \bar{w}_i\ f_i = \frac{w_i}{w_1 + w_2}, i = 1,2 \tag{10}$$

Layer 4: Every node i of this layer is the adaptive node, the output is

$$O_{4,i} = \bar{w}_i\ f_i = \bar{w}_i(p_i x_1 + q_i x_2 + r_i), i = 1,2 \tag{11}$$

Layer 5: The node of this layer computes the overall output as the summation of all the incoming signals.

$$O_{5,i} = \sum_i \bar{w}_i f_i = \frac{\sum_i w_i f_i}{\sum_i w_i}, i = 1,2 \tag{12}$$

ANFIS LearningAlgorithm. In order to minimize the error between the ANFIS output and the targets value, in this paper, a hybrid algorithm is employed, which is used for identification of the premise and consequent parameters. In the forward pass of learning algorithm, functional signals go forward till layer 4 and the consequent parameters are identified by the least-squares (LS) estimator. In the backward pass of the hybrid learning algorithm, the error rates propagate backward and the premise parameters are updated by the gradient descent.

ANFIS Flux Linkage Model. As discussed above, modeling of flux linkage characteristics can be grouped as a nonlinear function approximation problem. To solve this problem, an ANFIS based approximator was adopt for modeling. The ANFIS under consideration has two-input valuables rotor position (θ) and current (i), and one-output valuable flux-linkage (ψ). The input-output training data is based on the flux linkage characteristics obtained from EMEI. The corresponding multilayer architecture of ANFIS is shown in Fig. 4, which is composed of the parameters as listed in table.1.

Table 1. The architecture and the training parameters of ANFIS model

Number of membership functions for each input	7
Number of fuzzy rules	49
Number of nodes	131
Number of linear parameters	147
Number of nonlinear parameters	42
Total number of parameters	189
Number of training data pairs	336

By using the hybrid learning algorithm, the error between the desired output ψ and the actual output of ANFIS are evaluated until the estimation goal is reached. After training, the mapping of the estimated flux linkage characteristics can be obtained.

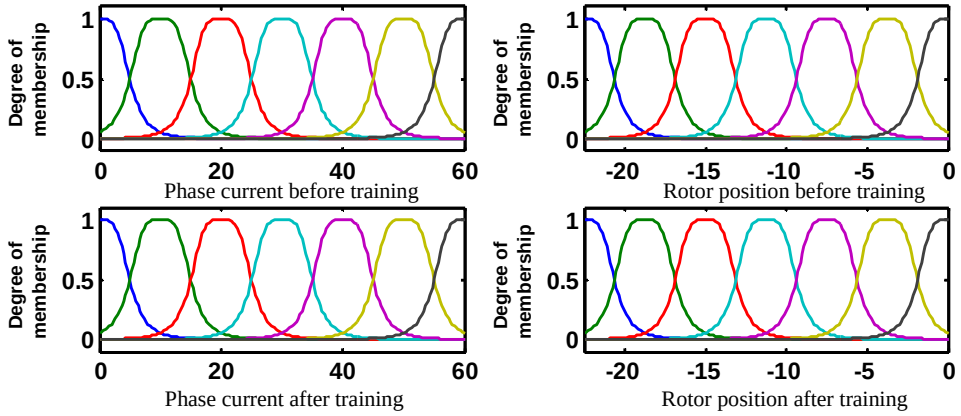

Fig. 5 Membership function adjustment of the input valuables

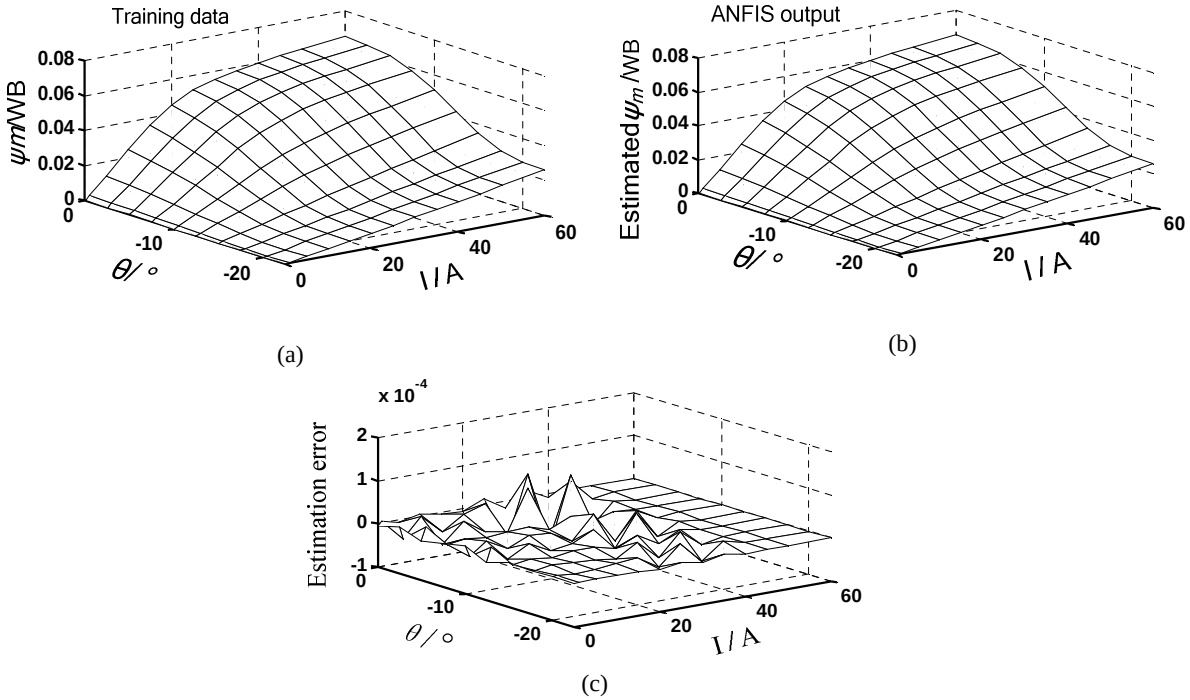

Fig. 6 The modeling results based on ANFIS (a) main winding flux linkage; (b) flux linkage obtained from ANFIS model; (c) the estimation error

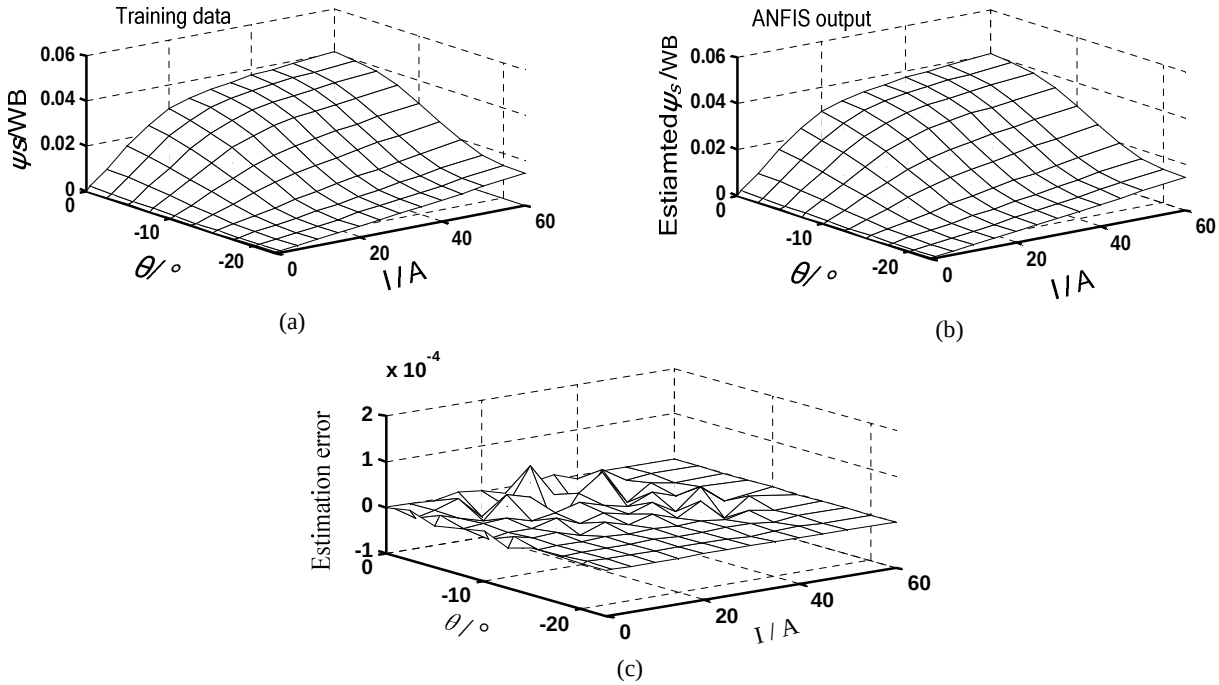

Fig. 7 The modeling results based on ANFIS (a) suspended winding flux linkage; (b) flux linkage obtained from ANFIS model; (c) the estimation error

The ANFIS modeling results are shown in Fig. 5-Fig. 7. Fig. 5 illustrates the self adjustment process of the inputs membership functions. The mapping surface of estimated flux-linkage of main winding and suspended windings are shown in Fig. 6(b) and Fig. 7(b), which were compared with the real value, and the estimation error mapping surface are shown in Fig. 6(c) and Fig. 7(c) respectively. It is clearly that the ANFIS model can approximate the real flux characteristics with great accuracy. As compared with the analytical nonlinear modeling method proposed in [8], the ANFIS model has many comparable advantages in types of modeling performance, which is summarized in Table. 2 and fully verified this modeling algorithm.

Table. 2 Comparison of the analytical model and ANFIS model

Performance type	Sub-regional model	ANFIS model
Model free	No	Yes
Precision	good	Very good
Modeling complexity	More	Less
Memory requirement	More	Less
Time consuming	More	Less
Robustness	Low	High
Adaptability	No	Yes
Convergence rate	Slow	Fast
Generalization	Good	Very good

Summary

In this paper, the flux linkage characteristics of main winding and suspended windings were calculated using EIEM by EFE based 3-D finite element analysis. Based on the calculated data, an ANFIS based model for nonlinear modeling of BSRM is investigated. The modeling results are presented and compared with the analytical methods, which indicated that ANFIS

is an ideal candidate for accurately modeling the electro-magnetism characteristics of BSRM. This will provide theoretical basis for the analysis, design and control of BSRM.

References

[1] Z. Q. Deng, G. Yang, Y. Zhang: Proceeding of the CSEE, 2005, 25(9), p. 139-146 (in Chinese).

[2] N.K.Sheth and K.R.Rajagopal: IEEE Trans. on Magnetics, vol.41, No.10, pp: 4069 – 4071, Oct 2005

[3] K. Vijayakumar, R. Karthikeyan, S. Paramasivam: IEEE Trans. on Magn., Volume: 44, Issue:12 On page(s):4605-4617, Dec.2008

[4] K.M. Rahman, S. Gopalakrisnan, B. Fahimi, A.V. Rajarathnam, M. Ehsani: IEEE Trans. on Industry Applications, vol.37, No.3, pp: 904-913, May/June 2001.

[5] T. Lachman, T. R. Mohamad and C. H. Fong: IEE Proceedings-Electric power applications, vol.151. No.1, page(s) 53-60, Jan 2004.

[6] J. Cai, Z. Q. Deng, Z. Y. Liu: in Proc. 25th IEEE Annual Applied Power Electronics Conference and Exposition, Palmspings, 2010, p. 1018-1025.

[7] Z. Y. Liu, S. S. Wang, and Z.Q. Deng: in Proc. Int. Conf. Electrical Machines and Systems, Wuhan, 2008, p. 439-443.

[8] J. Cai, Z. Q. Deng, Z. Y. Liu: in Proc. Int. Conf. on Applied Superconductivity and Electromagnetic Devices, Chengdu, 2009.